JOURNAL OF CRITICAL REVIEWS

ISSN- 2394-5125 VOL 06, ISSUE 06, 2019

RELEVANCE OF TEMPERATURE DISTRIBUTION FOR MICROSTRUCTURE AND MECHANICAL PROPERTIES OF SHIELD METAL ARC WELDED DUPLEX STAINLESS STEEL

Harish Kumar Arya,
Assistant Professor, Mechanical Engineering,
Sant Longowal Institute of Engineering & Technology, Longowal
Email- arya.iitr@gmail.com

Deepti Jaiswal,
Assistant Professor, Mechanical & Automation Engineering,
Indira Gandhi Delhi Technical University for Women, Delhi
Email-deeptijaiswal2007@gmail.com

Lucky,
Research Scholar, Sant Longowal Institute of Engineering & Technology,
Longowal, Sangrur, 148106
Email-lucky127@gmail.com

ABSTRACT: We evaluated the influence of a metal's initial high temperature on the microstructures and mechanical characteristics of a single-pass arc-welded steel plate. With metal preheat at 200o C, it was discovered that hardness qualities surrounding the heat-affected zone (HAZ) increased. Still,metal's toughness and tensile strength decreased with an initial elevated temperature of welded specimens. It has been demonstrated that, when welded steel microstructures are compared to base metal microstructures, the mechanical characteristics of the welded steel are more affected by the initial increased temperature than the base metal.

KEYWORDS: Microstructures, Duplex stainless steel, arc–weld, GTA welding, heat–affected zone, Electron beam welding, preheat, fusion zone, Mechanical properties, Heat treatment

INTRODUCTION:

In this study, the effects of microstructure, thermal history and heat input, and some other critical welding parameters, such as velocity and voltage, on the mechanical and physical properties of the welded alloy were studied using a welding simulation package for MIG welding of Al 6063 alloy. The following are the main findings of the empirical research and simulation: Increased welding speed leads to increased hardness, tensile strength, and yield stress for 6063 aluminium alloys. As arc voltage rises, the numbers above fall. A good agreement was found between the modelling and actual measurements of the alloy using temperature gradients and welding-induced stress fields. According to the findings of the FEM, the deformed zones extended up to 10 mm along the weld centerline. This virtually matched the empirical finding of 12 mm, which was almost identical. The fusion line was where compressive thermal stresses were generated. To further illustrate this point, a comparison of simulation results with actual data showed that the residual stress on our desired model is compressive between 4 and 11 mm from the weld centerline and tensile beyond that point. The huge heat sink phenomena prevented the parent metals from being fused at the start of the welding, resulting in thresholds in this respect, according to the FEM

findings and real-life temperature data. − It was found that the source metals had been mildly heated (partially annealed) during the welding, as shown by the microstructure and microhardness tests. The microstructure pictures showed that the agglomerated, overaged -Mg2Si phases in the HAZ and the pseudo-plate-like -AlFeSi precipitates in the fusion zone were precipitated alongside the smaller and coarser -Mg2Si. According to projections (based on the TTT curve) and several pieces of literature, 6063 Al sheets had a lesser quantity of -Mg2Si than 6061 Al sheets, which was following the results. − We were able to predict the involved phases and the mechanical behaviour of weldment because of in-situ temperature measurements of the fusion zone and the HAZ. These curves show how cooling rates may lead to precipitation of '-Mg2Si from the HAZ and beyond, for example, as represented by the TTT curves.

LITERATURE REVIEW:

Fourie and Robinson (1990) This study examines the differences between these two alloy types in their solidification and transformation properties (Austenitic stainless steel and duplex stainless steel). Duplex stainless steels solidify in the ferrite mode, whereas austenitic stainless steels solidify in the austenitic or austenitic-ferity modes. The austenite phase is generated during the solid-state transition that occurs in duplex stainless-steel weldments. Low heat inputs in duplex weldments cause substantial volume fractions of ferrite and severe precipitation of chromium nitrides, negatively impacting mechanical and corrosion characteristics. Welding duplex stainless steel requires significant heat inputs to enable austenite to reform long enough for the welds to cool. [3] [6].

Muruganet al. (2001) This research describes the heat cycles and transverse residual stresses in the weld pads of stainless steel AISI type 304 and low carbon steel with thicknesses of 6,8 and 12mm welded by Manual metal arc welding, respectively. For residual stress measurements, X-ray diffraction was utilised. It is observed that with increasing number of passes, peak tensile residual stresses on the root side of the weld pads decreases in magnitude and increases in magnitude on the top side. Due to stainless steel's reduced thermal conductivity, even with a lower heat input, the peak temperatures of stainless steel weld pads (closer to the weld line) are greater than those of low carbon steel weld pads.

Muthupandi et al. (2003) The microstructure and characteristics of duplex stainless steel welds were studied by these researchers [4][5]. Due to the high cooling rates involved with welding, the ferrite-austenite is often disturbed in DSS weld metals. The weld metal composition or the heat input must be regulated to obtain the required ferrite-austenite balance and, thus, characteristics.

Kolhe and Datta(2008) Using trinacular metallurgical microscopy, with onix vision video, this research investigates the microstructure, phase analysis, and mechanical characteristics of SA weld metal multipass joints and the HAZ of 16mm thick mild steel plates. In addition to a high-resolution camera, the system includes image analysis software. It was discovered that the CVN value of the fusion zone increased with the rise in ferrite content in the microstructure and decreased with the increase in maretensite-austenite concentrations in the microstructure [7].

Adedayo and Momoh (2010) In this article, the microstructure and mechanical characteristics of a single pass arc welded mild steel plate were examined about the beginning temperature, with no preheat, preheat at 100oC, and preheat at 200oC. A reduction to the base metal value is seen in all welding situations, although the HAZ has the highest hardness,

ISSN- 2394-5125 VOL 06, ISSUE 06, 2019

tensile strength, and toughness in mild steel plates. A difference in microstructure between the heated and unheated specimens is evident, with the preheated specimen displaying evidence of bainite precipitation. [8][9] The hardness of mild steel is reduced by heating it before welding.

OBJECTIVES:

Objectives of the study are-

- To study the mechanical properties (tensile and impact strength) of welded samples
- To study the microhardness of welded samples
- To study the bead profile and microstructure of welded samples

Microstructure:

A secondary electron SEM (Scanning electron microscope) image of a weld bead with various regions marked on it is shown in Figure 1 as an optical micrograph of the solution annealed sample and a weld bead with a weld zone in cap pass (region III) and a root pass (interface between the cap and the weld zone in region IV) in the weld zone (region V) (root pass). Also shown is the area where micro and hardness originate. There are 50 percent austenite and 50 percent ferrite in the SDSS-50 (Super duplex stainless steels), with the microstructure various thicknesses of austenite and ferrite as well as grains that are elongated in the original rolling direction of the hot rolled sheet. The heat input during welding has a significant impact on the microstructures and mechanical characteristics of weldments.

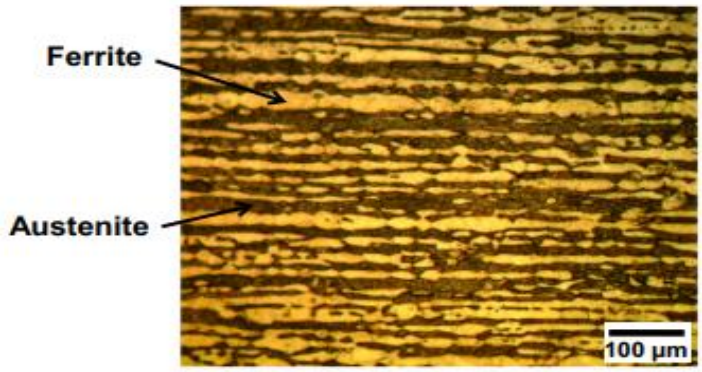

(a)

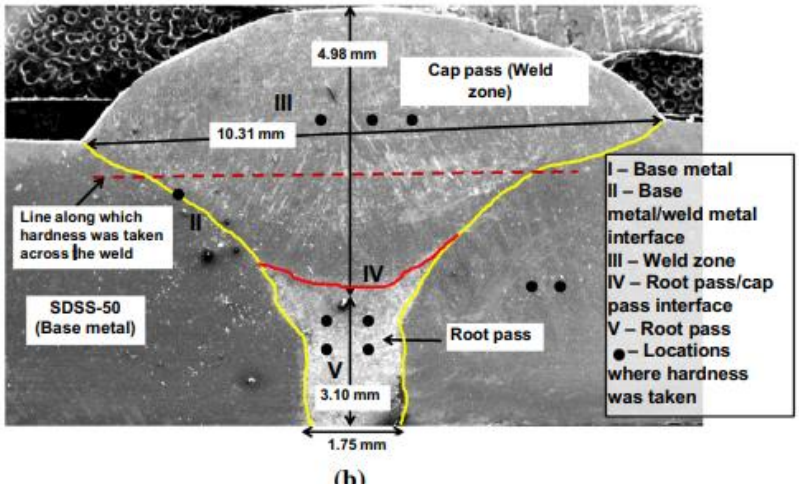

(b)

Figure-1: a) Initial solution annealed SDSS-50 sample seen via an optical microscopeand b) secondary electron SEM picture of the bead with different sections indicated on it.

When the heat input increases, the weld bead's width and penetration expand along with it, and the HAZ at the fusion boundary widens as well. Weld metal (WM) microstructure in the cap pass zone for both heat inputs is shown in Figure 2. (LHI and HHI). The microstructure properties of Widmanstatten austenite (WA), intergranular austenite (GBA) and intra-granular austenite (IGA) are important for both the heat inputs. Widmanstatten austenite (WA) begins to develop at d-ferrite grain borders during cooling, and subsequently increases inside the grain when austenite crystallises at grain boundaries. Additionally to GBA and WA, IGA can nucleate and develop inside d–ferrite grains if sufficient time for diffusion occurs (depending on the cooling rate)... (Fig. 2d). GBA and WA dominate the final microstructure because they require less under-cooling to develop than IGA (the driving force). Figure 2a, b shows that when heat input rises during the SMAW process, grain size decreases in the fusion zone. To our knowledge, no intermetallics were found in the weld zone for either heat input. When it comes to high-energy density techniques like electron beam welding (EBW), Cr2N precipitates are more likely to form, according to a study (GTAW, SMAW etc.).

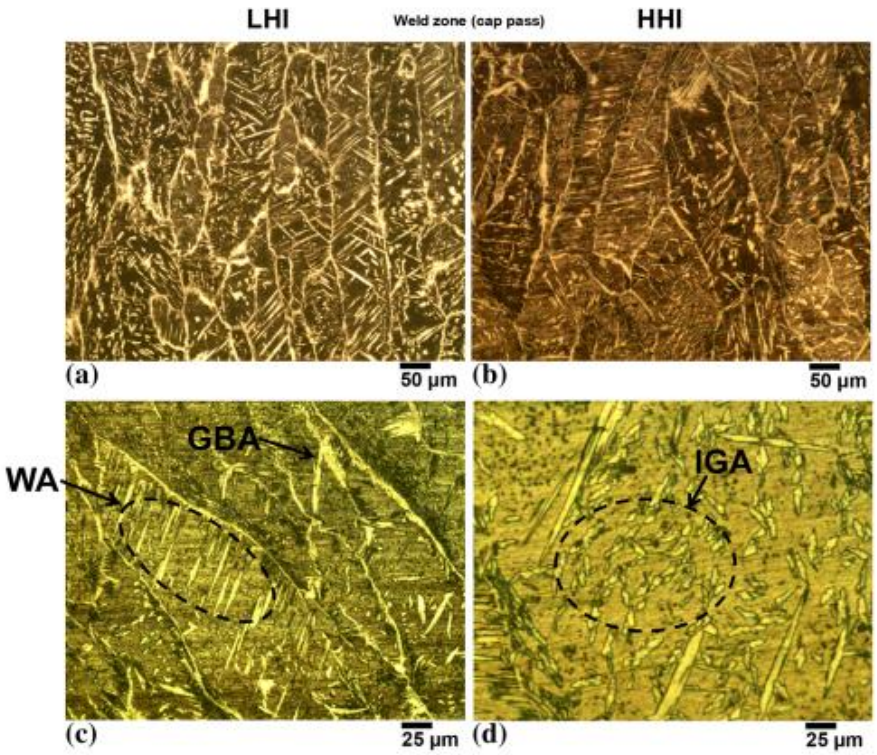

Figure-2: The weld zone's optical microstructures (cap pass). a, b are at low magnification and c, d are at higher magnification

The weld zone did not have any Cr2N precipitations in this research either. As a result of the faster cooling rate at lower heat input, the weld metal will have considerably steeper thermal gradients. Fine dendritic structure is the outcome of this (restricted growth of dendrites). As a result of a slower cooling rate at HHI, dendrites are coarser than at LHI (Fig. 2). It has been observed that austenite forms within d-ferrite and spreads across the fusion zone at a rapid rate of cooling such that no further transformation can take place in the process. In the cap pass zone, the average ferrite concentration is roughly 72% and

ISSN- 2394-5125 VOL 06, ISSUE 06, 2019

austenite is approximately 28%. Figure 3 depicts the root pass's microstructure for the two heat inputs. In addition, the total ferrite content in the microstructure is about equivalent to 67 percent, which is significantly larger than the bottom limits (* 30 percent) for acceptable mechanical qualities.

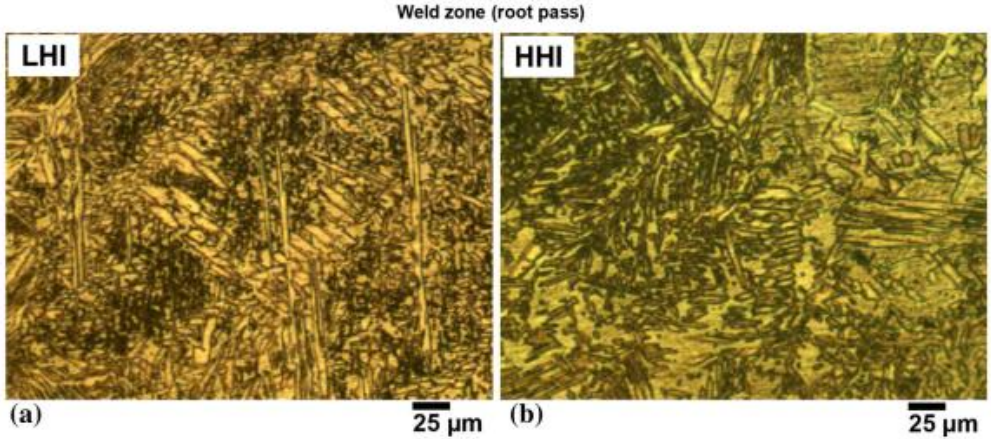

Figure-3:Weld zone root pass microstructures for LHI and HHI samples

As the d-ferrite cools more slowly, it has more time to undergo c-transformation, resulting in longer root passes. The different heat cycles in the two locations are to blame for the 11 percent ferrite content differential between the cap pass and root pass of an LHI weld. Imaging of optical microstructures and secondary electron images (SEM) are shown in Figures 4 and 5, respectively, for the WM/BM interface. In terms of heat inputs, the HAZ is quite small. It is 120–130 lm broad for LHI and 138–145 lm wide for HHI, depending on the area, and only contains one layer of big grain size. Understanding the heat cycle of the HAZ may explain why the grain dispersion is so small. The ferrite solvus may have been surpassed by a few degrees in HAZ, preventing any grain development. Because of the lack of grain development in the HHI weldments, the HAZ's breadth is generally a function of the amount of heat applied to the welds. A greater solvus of ferrite may be to blame, as this results in a narrow band of ferritic material running parallel to grain boundaries. HAZ PTA (Figure 5) is typically useful because it inhibits grain development. An acicular austenite, PTA, may be seen in some areas of HAZ seen in Figure 5. To achieve a good combination of mechanical and corrosion characteristics, it is critical to optimise the fusion zone ferrite composition. Extremely low ferrite content can lead to a decrease in strength, whereas high ferrite content (>75%) can lead to a decrease in corrosion resistance and impact strength.

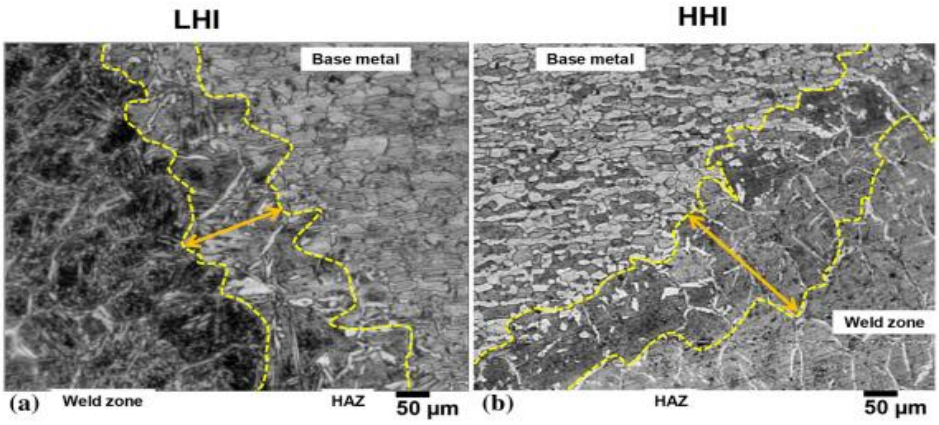

Figure-4:LHI and HHI samples were analysed for optical microstructures of the heat affected zone (HAZ).

ISSN- 2394-5125 VOL 06, ISSUE 06, 2019

Weld dilution and ferrite content must be kept under strict control, and this is mostly accomplished by monitoring and adjusting the various aspects of the welding process. Both the root and cap passes of the SMAW with ER2595 electrode have ferrite concentration that is within the permissible range (shown in Table 3). The amount of ferrite in the weld (cap pass) zone reduces as the heat input increases. The weldment cooling rate has changed as a result. The austenite transition from the d-ferrite is accelerated by fast cooling compared to slow cooling (HHI). High heat input weldments also have a greater ferrite concentration than low heat input weldments. Ferrite volume percentage in the HHI weld (cap pass) is 70% for ER2595, whereas in the root pass it is * 67%. The higher ferrite concentration in the weld zone is due to grain development in the HAZ. Ferrite content likewise reduces when one moves from the cap pass to the root pass.

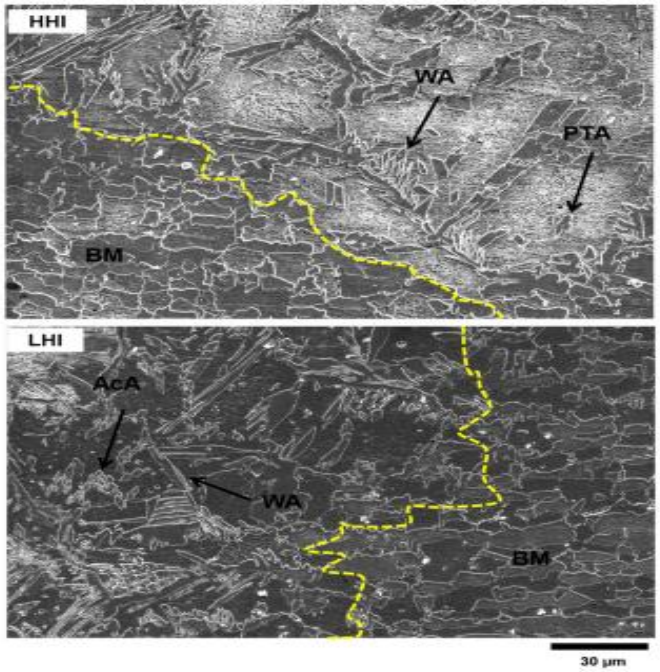

Figure-5:HAZ for LHI and HHI sample secondary electron SEM images

EXPERIMENTAL PROCEDURE:

An IS 3589 GR 330 Class A91A duplex stainless steel was selected as a starting point. The 100 x 150 mm and 10 mm thick test plates have been used in the experiment. plates with a 1 mm root face have one 60 degrees V-groove cut into it. Using shielded metal arc welding with a root gap of 2 mm between two plates, a final weld pad of 202 x 150 mm and 10 mm was created for the Butt joint sample. It was necessary to remove all potential contaminants, including rust, scale, dust, oil, and moisture (among others), from the edges of the weld metal before welding to reduce the risk of a welding fault. After the plates had been tacked together, SMAW weld passes were performed using the conditions listed in table 3.1, with an interpass temperature of roughly 1500C maintained before the second pass was delivered. The specimen was neither preheated nor post-heated. A skilled welder performed the multipass welding. Transient temperatures during welding were measured using K-type thermocouples with a 1.5mm tip diameter. This is the most often used thermocouple for general purpose applications, Type K (Chromel-alumni). In addition to being affordable, it comes in a broad range of probes. They vary from -2000C to +13500C in temperature. Two thermocouples were positioned at 20mm intervals from the weld pad centre on the plate in

ISSN- 2394-5125 VOL 06, ISSUE 06, 2019

the central section, at midplane level. Weld pad temperatures were recorded at various distances from the centre line of the weld pad on one of its side plates. As a result, the four thermocouples were inserted into base plate holes, and welding beads were then placed on the other side. The digital metre was linked to each thermocouple to record the temperature at the same time interval.

Figure 6 shows the dimensions of the plates used in the tests and the locations where thermocouples were attached. We labelled our samples A (low heat input), B (medium heat input), and C for the sake of clarity for the reader (High heat input). This sample's butt welded joints were manufactured using the method parameters listed in table 1.

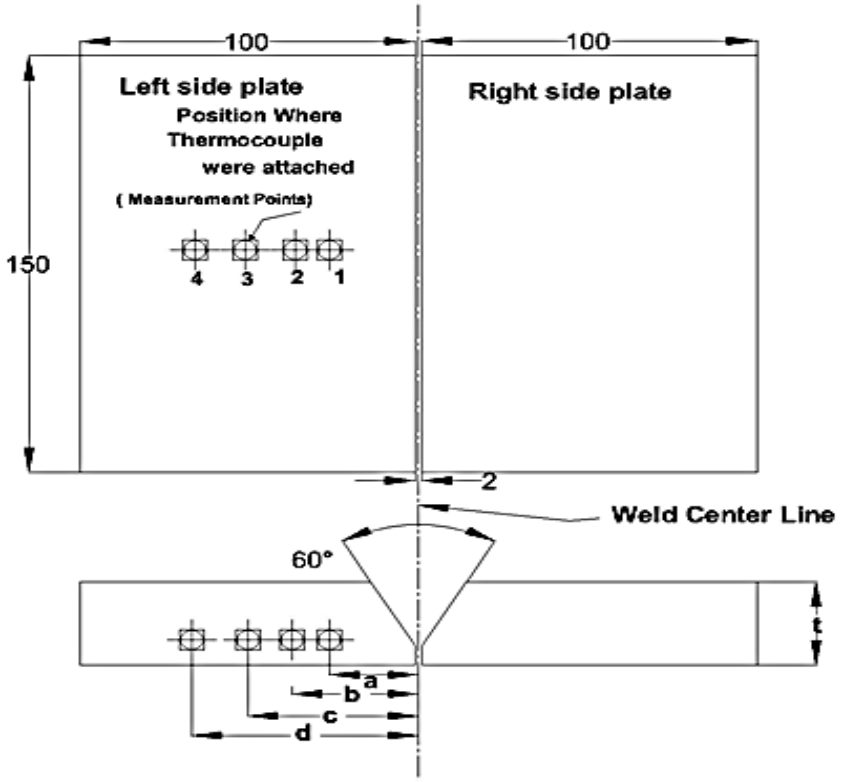

Sample No:	Thickness of plate (t)	A	B	c	d
A	10	20	40	60	80
B	10	20	40	60	80
C	10	20	40	60	80

All dimensions are in mm.

ISSN- 2394-5125 VOL 06, ISSUE 06, 2019

Figure-6: Dimensional details of plates used for welding in the experiments.

Sample no	Pass	Current (A)	Voltage (V)	Welding Speed (mm/s)	Heat input per unit length per pass (KJ/mm)	Total heat input per unit length of weld (KJ/mm)	Average heat input per unit length of weld (KJ/mm)
A (low heat)	First	90	37.2	3.68	0.6823	2.7018	0.675
	Second	90	37.2	3.77	0.6660		
	Third	90	37.2	3.73	0.6731		
	Fouth	90	37.2	3.69	0.6804		
B(medium heat)	First	105	40.7	3.67	0.8733	3.4418	0.860
	Second	105	40.7	3.72	0.8615		
	Third	105	40.7	3.77	0.8501		
	Fouth	105	40.7	3.74	0.8569		
C (high heat)	First	120	45.3	3.78	1.0785	4.375	1.094
	Second	120	45.3	3.72	1.0959		
	Third	120	45.3	3.70	1.1018		
	Fouth	120	45.3	3.70	1.1018		

Table 1: Process parameters used for fabricating butt welded joints

RESULTS AND DISCUSSION:

- **Micro Hardness Analysis:**

A material's resistance to being scratched or eroded is one way to measure hardness. An Akashi micro vicker harness tester (MVK-H2) with a test load of 0.5 kg was used at the Institute for Auto parts & Hand tools technology, Ludhiana, to conduct a micro hardness test. The microhardness tester used a diamond indenter to measure the hardness of the welds. Vickers hardness values may be automatically calculated (VHN). A hardness test was used to distinguish three distinct zones from the fusion boundary to the base metal of shielded metal arc welded joints. Hardness differences concerning the distance from the weld centreline were shown using hardness profiles obtained from welding specimens. It is possible to determine the metallurgical changes that have occurred due to welding by measuring hardness. Testing for weld hardness is necessary to guarantee that the weld metal meets or exceeds the parent metal's strength requirements.

A cross-sectional microhardness test was conducted on samples A, B, and C, starting at the weld centre line and moving toward the base metal. Weld sample A, B, and C's microhardness in cross-section from the weld centre line to base metal are presented in tables 2 to 4. It was shown that the hardness value of the heat impacted zone (HAZ) decreases as the heat input rises in samples A, B, and C. Figure 7 shows a high hardness value in the low heat input weld zone, or weld sample A. There is a possibility that the equiaxed grains might be to blame since the inner zone shows grains that have cooled more slowly.

Distance (in mm)	1	2	3	4	5	6	7	8	9	10	11
(VHN)	275	270	293	279	270	268	265	264	265	260	272

Table 2: Microhardness of weld **sample A** across cross-section from weld centre line towards base metal

ISSN- 2394-5125 VOL 06, ISSUE 06, 2019

Distance (in mm)	1	2	3	4	5	6	7	8	9	10	11
(VHN)	261	262	286	270	272	275	279	272	260	276	274

Table 3: Micro hardness of weld **sample B** across cross section from weld centre line towards base metal

Distance (in mm)	1	2	3	4	5	6	7	8	9	10	11
(VHN)	280	282	287	282	293	295	289	284	285	280	281

Table 4: Micro hardness of weld **sample C** across cross-section from weld centre line towards base metal

Variation of hardness with the distances from the weld centre line towards the base metal has shown in graph in Fig.7.

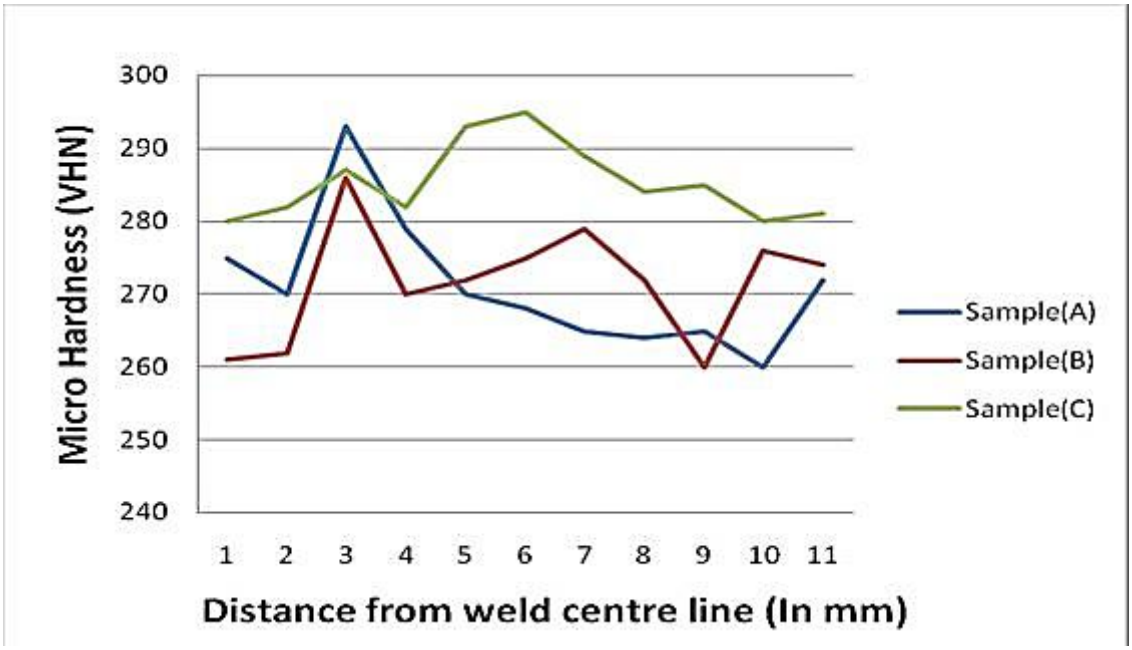

Figure-7: Micro hardness graph of weld samples across cross section

CONCLUSION

Weld metal devoid of columnar grains was created with a low heat input (0.675 KJ/mm). Columnar dendrites were formed in the weld metal due to an increase in heat input. Because the cooling rate is higher (0.346 oC/Sec) at low heat input, steep thermal gradients are established in the weld metal, giving the dendrites less time to grow. Conversely, at high heat input (1.094 KJ/mm), the cooling rate is slow (0.0190 oC/Sec), which gives the dendrites plenty of time to grow further into the fusion zone and reach their maximum diameter.. A larger bead and penetration area may be seen as the temperature rises. This is because when the heat input rises, the cooling rate decreases. A microstructure investigation of all the weldments demonstrates that the HAZ (heat affected zone) has a fine grain structure with minimal dendrites under low heat input. Has with fine grain structure at low heat input have the highest tensile strength and harness. At 100 X, the weld metal has an austenitic, ferritic structure with some austenite patches, whereas the weld metal of medium heat input has a

mixed grain structure with equiaxed grains. Low and high heat input welded junctions have less impact strength/toughness than austenite patches in the HAZ. There has been partial dendritic development in the HAZ and mixed grains structure in the weld metal at high heat input, revealing unevenly cooled grains and partial dendritic formation. In contrast to low and medium heat input weldments, there is a coarse grain structure. The welded joint's poor tensile strength and hardness are HAZ is due to the unevenly cooled grains with partial dendrites/coarse grain structure.

REFERENCES:

1. Adedayo, S.M. and Momoh, S.O. (2010), 'Effect of initial elevated metal temperature on mechanical properties of an Arc welded mild steel plate', *Indian Journal of Science and Technology*, vol. 3, no. 12.

2. Attarha, M.J. and Sattari-Far, I. (2011), 'Study on welding temperature distribution in thin welded plates through experimental measurements and finite element simulation', *Journal of Materials Processing Technology*, vol. 211, pp. 688-694.

3. Cunat, P. (2004), 'Alloying elements in stainless steel and other chromium containing alloys' ,*International Chromium Development Association*, ICDA, 45.

4. Ciofu, F., Nioata, A. and Luca, L. (2010), 'Duplex stainless steel corrosion resistance', *Fascicle of Management of Technological Engineering*, vol. 9.

5. Fourie, J.W. and Robinson, F.P.A.(1990), 'Literature review on the influence of weld-heat inputs on the mechanical and corrosion properties of duplex stainless steels', *J.S.Atr. Inst. Min.Metall*, vol. 90, No. 3,pp. 59-65.

6. Kordatos, J.D., Fourlaris, G. and Papadimitriou, G. (2001), 'The effect of cooling rate on the mechanical and corrosion properties of SAF 2205(UNS 31803) duplex stainless steel welds', *Scripta Mater,* vol. 44, pp.401-408.

7. Kolhe, P. and Datta, C.K. (2008), 'prediction of microstructure and mechanical properties of multipass SAW' ,*Journal of Materials Processing Technology*, vol. 197, pp. 241-249.

8. Khanna, O.P. (2009) Physics of welding. *Welding Technology.* 1st ed. New Delhi: Dhanpat Rai, pp. 539-567.

9. Kumar, S. and Shahi, A.S. (2011), 'Effect of heat input on the microstructure and mechanical properties of gas tungsten are welded AISI 304 stainless steel joints', *Materials and Design,* vol. 32, pp. 3617-3623.